

Quercetin induces protective autophagy and apoptosis through ER stress via the p-STAT3/Bcl-2 axis in ovarian cancer

Y. Liu^{1,4} · W. Gong² · Z. Y. Yang¹ · X. S. Zhou¹ · C. Gong¹ · T. R. Zhang¹ · X. Wei¹ · D. Ma¹ · F. Ye³ · Q. L. Gao¹

© Springer Science+Business Media New York 2017

Abstract Quercetin (3,3',4',5,7-pentahydroxyflavone, Qu) is a promising cancer chemo-preventive agent for various cancers because it inhibits disease progression and promotes apoptotic cell death. In our previous study, we demonstrated that Qu could evoke ER stress to enhance drug cytotoxicity in ovarian cancer (OC). However, Qu-induced ER stress in OC is still poorly understood. Here, we demonstrated that Qu evoked ER stress to involve in mitochondria apoptosis pathway via the p-STAT3/Bcl-2 axis in OC cell lines and in primary OC cells. Unexpectedly, inhibition of ER stress did not reverse Qu-induced cell death.

Further functional studies revealed that Qu-induced ER stress could activate protective autophagy concomitantly by activating the p-STAT3/Bcl-2 axis in this process. Moreover, the autophagy scavenger 3-MA was shown to enhance Qu's anticancer effects in an ovarian cancer mice xenograft model. These findings revealed a novel role of ER stress as a "double edge sword" participating in Qu-induced apoptosis of OC and might provide a new angle to consider in clinical studies of biological modifiers that may circumvent drug resistance in patients by targeting protective autophagy pathways.

Keywords Qu · ER stress · Autophagy · Ovarian cancer · p-STAT3/Bcl-2 axis

Yi Liu, Wei Gong and Zongyuan Yang contributed equally to this work.

Electronic supplementary material The online version of this article (doi:10.1007/s10495-016-1334-2) contains supplementary material, which is available to authorized users.

✉ F. Ye
yeyuanbei@hotmail.com

✉ Q. L. Gao
qlgao@tjh.tjmu.edu.cn

¹ Cancer Biology Research Center, Tongji Hospital, Tongji Medical College, Huazhong University of Science and Technology, Wuhan, Hubei 430030, People's Republic of China

² Department of Oncology, XiangYang Central Hospital, Hubei University of Arts and Science, Xiangyang 441021, China

³ Neurosurgery Department, Tongji Hospital, Tongji Medical College, Huazhong University of Science and Technology, Wuhan, Hubei 430030, People's Republic of China

⁴ Department of Medicinal Chemistry, School of Pharmacy, Hubei University of Chinese Medicine, Wuhan, Hubei 430065, People's Republic of China

Introduction

Ovarian cancer (OC) is the fifth leading cause of cancer-related death among women and has the highest mortality rate of all gynecological malignancies in the United States [1]. The current barriers in patients with OC are that the cancer is undetectable at early stages, has a tendency to relapse, and is inclined to develop drug resistance. Currently, the standard treatment for OC is cytoreductive surgery followed by chemotherapy, with a devastating 5 year survival rate for all stages of ~47% [2]. This poor clinical outcome highlights the need for more efficacious targeted molecular therapies in this devastating disease.

Plant-derived bioactive compounds are newly recognized as alternates or adjunct therapies for various forms of cancer and have less toxicity than conventional anti-cancer drugs [3]. Qu, the most common flavonoid in many fruits and vegetables, has shown anticancer effects for many cancers including colon, breast, and ovarian

cancers [4–6], and has been approved in clinical trials for tyrosine kinase inhibition [4]. Although Qu has potential as an anti-cancer therapy, the underlying mechanisms are still not well understood regarding to OC.

Endoplasmic reticulum (ER) is responsible for protein translocation, protein folding, and protein post-translational modifications. Perturbations in ER function, a process named “ER-stress”, triggers the unfolded protein response (UPR), a tightly orchestrated collection of intracellular signal transduction reactions designed to restore protein homeostasis. ER stress can trigger the apoptotic machinery and ultimately lead to cell death under severe or chronic stress conditions, for instance, when adaptive responses are exceeded or a dysfunctional UPR is unable to correct the balance of ER stress [7]. Evidence for the role of ER stress-mediated cell death in a variety of diseases makes this process an attractive target for cancer therapy [8]. In our previous study, we demonstrated that Qu evoked ER stress to enhance drug cytotoxicity in OC [9, 10]. However, the mechanism of the anti-cancer activity of Qu-induced ER stress is poorly understood.

Autophagy, a stress-induced cell survival program that has long been known to remove dysfunctional organelles and/or proteins by shuttling them to the lysosome for degradation [11], can be activated by ER stress pathways, which is supported by numerous independent studies [12, 13]. However, the role of autophagy in cancer chemotherapy is still controversial. Cancer cells may utilize autophagy to survive in the hostile tumor microenvironment, suggesting deployment of therapeutic strategies to block autophagy for cancer therapy. On the contrary, high levels of autophagy might lead to cell death in cancers [14]. This phenomenon may depend on the varying nature of stress stimuli on cells and tissues. Qu has the potential to induce protective autophagy in gastric cancer through AKT-mTOR and hypoxia-induced factor 1 α signaling [15]. Although Qu was also demonstrated to induce autophagy in OC [3], there was no direct evidence to explain the exact role of Qu-induced autophagy. Therefore, we were determined to explore whether Qu-induced ER stress could evoke autophagy and its exact role in OC.

In this study, we found that Qu-induced ER stress acted bidirectionally involving apoptosis in OC via the p-STAT3/Bcl-2 axis and including the mitochondria apoptosis pathway and protective autophagy. Inhibition of autophagy could reverse this “side effect” of Qu. The above results let us reconsider the role of ER Stress in the treatment of ovarian cancer with Qu.

Materials and methods

Reagents and cells

The antibodies for Bcl-2, BAD, BAX, cytochrome C, Caspase-3, Caspase-4, Caspase-9, phospho-STAT3 (Tyr705), CHOP and GAPDH were purchased from Cell Signaling Technology (MA, USA). The antibodies for GRP78, horseradish peroxidase-conjugated anti-mouse IgG and anti-rabbit IgG were purchased from epitomics (abcam, USA). pEGFP-LC3 (human) (Plasmid 24920) and Human Bcl-2/pcDNA3 (Plasmid #19279) were purchased from Addgene (USA). The antibodies for Beclin 1, LC3B, ATG5 were purchased from Abcam (abcam, USA). Qu, Z-VAD-fmk, static and 3MA were purchased from Sigma–Aldrich (MO, USA). Tauroursodeoxycholic acid (TUDCA), salubrinal and sp600125 were purchased from Calbiochem (San Diego, CA). 3-ethoxy-5,6-dibromosalicylaldehyde (3-E-5, 6-D) were purchased from Sigma (St. Louis, MO, USA). CAOV3 human ovarian cancer cells, from American Type Cell Culture (ATCC, Manassas, VA, USA) were grown and maintained in DMEM medium supplemented with 10% fetal bovine serum (FBS), 100 U/ml penicillin, 100 μ g/ml streptomycin and 25 μ g/ml amphotericin B. P#1, a primary ovarian cancer cell was isolated and identified as described [9], with a purity greater than 90% (data not shown). Cells were cultured at 37°C in a humidified incubator with 5% CO₂ and 95% air and were regularly examined using an inverted microscope.

MTT assay

The MTT assay was employed to examine the effects of Qu on the proliferation of ovarian cancer cells. Briefly, the cells were seeded in 96-well plates at 5×10^3 cells/well in 200 μ l medium. Then, the cells were treated with various concentrations of Qu and cultured for 48 h. At the end of the culture period, the MTT solution (0.5 mg/ml in 20 μ l PBS) was added to each well and incubated for 4 h at 37°C. An enzyme-labeled instrument (Thermo) measured the absorbance of each well at 570 nm. The data were calculated from three independent experiments, each performed in sextuplicate.

Colony-forming assay

Cells were seeded into 6-cm dishes in triplicate at a density of 1000 cells per dish. The cells were pretreated with Qu in different concentrations for 48 h. Then, the medium was changed and the cells were incubated for another 14 days in a humidified incubator at 37°C. Colonies were fixed with 4% paraformaldehyde, stained with 0.5% crystal violet and counted.

Annexin V-FITC-propidium iodide assay

An Annexin V-FITC apoptosis kit (KeyGEN Biotech, Nan-Jing, China) was used to determine the number of apoptotic cells according to the manufacturer's instructions. Briefly, cells were grown in 12-well plates, after 80–90% confluence, different treatments were applied to the cells. The cells were harvested after the indicated time, washed twice with ice-cold PBS and resuspended in 500 μ l of binding buffer. Then, 5 μ l Annexin V-FITC and 10 μ l propidium iodide were added and the mixture was incubated in the dark at 4 °C for 10 min. A total of 10,000 events per sample were analyzed. Annexin V-FITC positivity was calculated with a FACS Calibur flow cytometer (BD Biosciences, Franklin Lakes, NJ, USA) using WinMDI 2.8 software.

Cell survival assay

An Annexin V-FITC apoptosis kit (KeyGEN Biotech, Nan-Jing, China) was used to determine the number of apoptotic cells according to the manufacturer's instructions. Briefly, cells were grown in 12-well plates, after 80–90% confluence, different treatments were applied to the cells. The cells were harvested after the indicated time, washed twice with ice-cold PBS and resuspended in 500 μ l of binding buffer. Then, 5 μ l Annexin V-FITC and 10 μ l propidium iodide were added and the mixture was incubated in the dark at 4 °C for 10 min. A total of 10,000 events per sample were analyzed. Annexin V-FITC negative was calculated with a FACS Calibur flow cytometer (BD Biosciences, Franklin Lakes, NJ, USA) using WinMDI 2.8 software.

Western blot analysis

Cells were harvested and washed twice with cold-PBS and lysed in lysis buffer (50 mM Tris-HCl pH 8.0, 150 mM NaCl, 1% NP-40) containing 1mM phenylmethylsulfonyl fluoride (PMSF) and protease inhibitor cocktail for 30 min on ice. After centrifugation at 12,000 rpm for 15 min, the supernatant was collected. The total protein concentration was determined using a BCA protein assay kit. Briefly, 50 μ g of total protein from each sample was loaded, separated by SDS-PAGE and transferred to a polyvinylidene difluoride (PVDF) membrane. Transferred membranes were blocked for 1 h with TBS containing 0.1% Tween-20 and 5% BSA at room temperature and then incubated overnight with an appropriate dilution of the primary antibody at 4 °C. After washing three times with TBS containing 0.1% Tween-20, membranes were incubated with the corresponding HRP-linked secondary antibody. Finally, the immune complexes were visualized via fluorography using an enhanced ECL system (Pierce, USA).

Co-immunoprecipitation

CAOV3 and P#1 were treated with or without Qu for 48 h. Proteins were extracted using lysis buffer (50 mM Tris-HCl pH 8.0, 150 mM NaCl, 1% NP-40 and 2 mM EDTA). Protein samples were immunoprecipitated with Bcl-2, Beclin 1 antibodies or irrelevant IgG at 4 °C overnight. Then, the immunoprecipitated protein was pulled down with 20 μ l protein G-Sepharose at 4 °C for 4 h. The beads were then washed four times with lysis buffer before SDS-PAGE electrophoresis.

Transfection of siRNA

CHOP, Beclin 1, ATG5, Bcl-2 and non-targeting control siRNAs were purchased from Santa Cruz Biotechnology. Cells were transfected with siRNAs using Lipofectamine 2000 (Invitrogen, USA), according to the manufacturer's instructions.

In vivo experiments

This study was performed with approval from the Committee on the Ethics of Animal Experiments in the Hubei province. All animal experiments were carried out in accordance with the Guide for the Care and Use of Laboratory Animals of Tongji Hospital in Hubei. 4–6 week old female nude athymic NOD/SCID mice were housed and maintained in laminar flow cabinets under specific pathogen-free conditions. CAOV3 human ovarian cancer cells (5×10^6 in 200 μ l volume of PBS) were injected via intraperitoneal injection (i.p.). Approximately 5 days after tumor implantation, the mice were randomized into four groups with eight mice/group and treated i.p. with 80 mg/kg Qu twice a week, 30 mg/kg 3MA twice a week, a combination of 30 mg/kg 3MA and 80 mg/kg Qu twice a week, or a vehicle control injected with the same volume of saline for 4 weeks. The tumor volume in the abdominal cavity of each mouse was assayed by in vivo bioluminescence imaging after the completion of the experiment.

Human ovarian cancer CAOV3 cells (5×10^6 in 100 μ l volume of PBS) were injected s.c. into the right supra scapula region of mice. Tumor volume was estimated using the formula $\text{volume} = \text{length} \times \text{width}^2 / 2$. Approximately 1 week after tumor implantation, when the tumor reached a mean group size of 50 mm³, the mice were randomized to four groups with six mice/group and treated with i.p. of 80 mg/kg Qu twice a week, 30 mg/kg 3MA twice a week, a combination of 30 mg/kg 3MA and 80 mg/kg Qu twice a week, or a vehicle control injected with the same volume of saline for 4 weeks. The tumor volumes were determined by caliper measurement every 4 days.

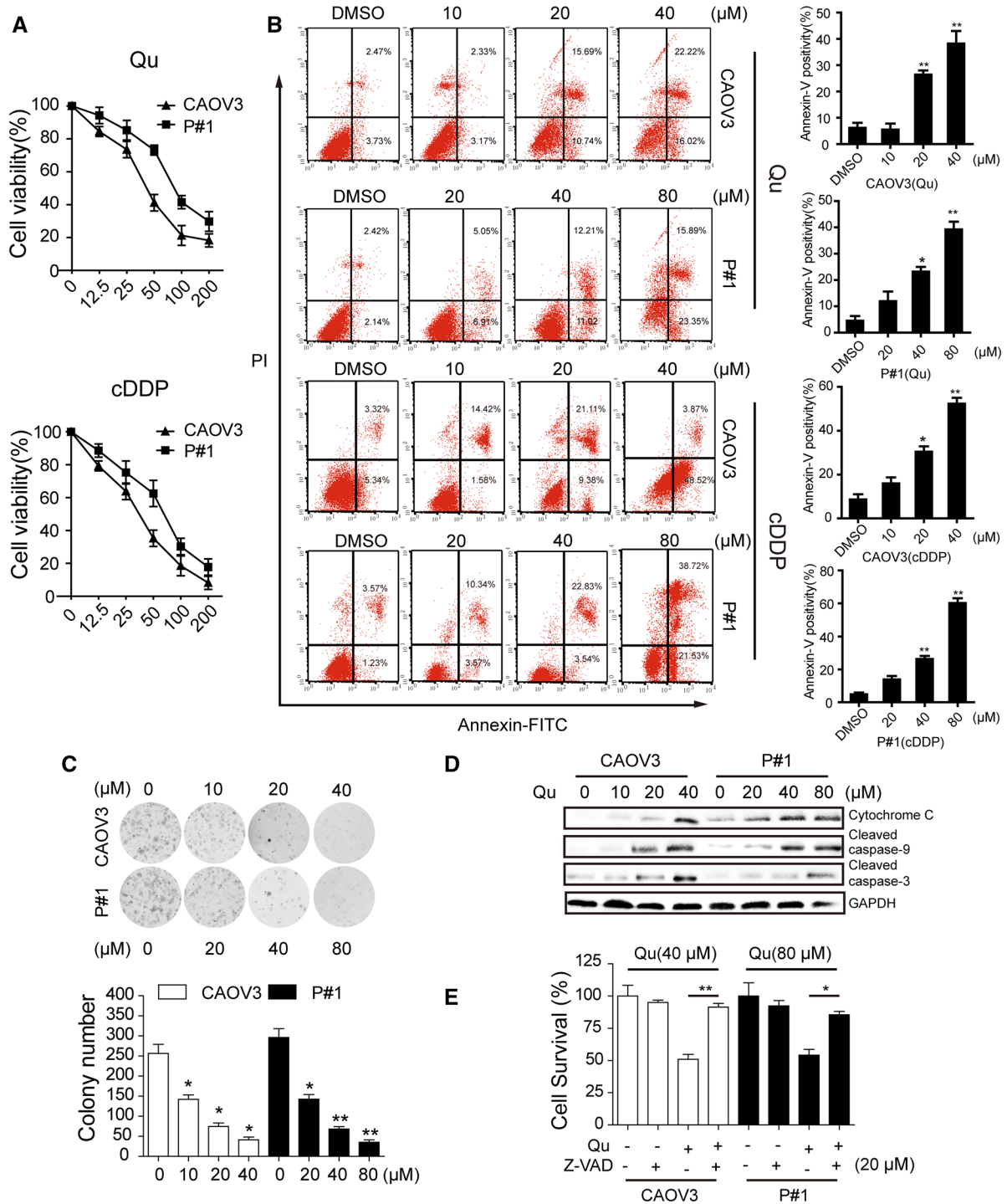


Fig. 1 Qu-induced apoptosis in ovarian cancer cells. CAOV3 and primary ovarian cell P#1 were treated with increasing concentrations of Qu for 48 h (a–d). **a** The cell viability rate was assessed using the MTT assay. **b** The apoptotic rate was analyzed by flow cytometry. **c** The effect of growth inhibition was measured by the violet staining assay, and photographs were taken at 14 days after quercetin interven-

tion. **d** Lysates were harvested and immunoblotted with cleaved caspase-3, cleaved caspase-9 and cytochrome C antibodies. **e** Cells were treated with DMSO (0.1%), Qu (40 μM for CAOV3 and 80 μM for P#1) in the absence or presence of 20 μM Z-VAD-fmk for 48 h, and the cell survival was analyzed by flow cytometry. The results were similar in at least three independent experiments. * $p < 0.05$. ** $p < 0.01$

Tumor tissue samples from mice were isolated for histopathological evaluations.

Immunohistochemical staining

After the mice were sacrificed, tumors were excised and stored in 5% formalin for 24 h; the tumors were then embedded in paraffin, sectioned, and subjected to immunohistochemical staining for GRP78, Beclin 1 and Bcl-2 expression using the streptavidin-peroxidase technique as described previously. Briefly, sections were deparaffinized and incubated with 3% H₂O₂ in distilled water to block endogenous peroxidase activity. After antigen retrieval, the sections were blocked with goat serum for 30 min and then incubated with a primary antibody overnight at 4 °C. After washing with PBS, the sections were incubated with horseradish peroxidase linked secondary antibodies for 30 min. After washing with PBS, the sections were developed in DAB solution until the desired staining intensity was achieved. Finally, the sections were counterstained with hematoxylin.

Statistical analysis

The data were expressed as means \pm SD of at least three independent experiments. Statistical analysis was performed using the SPSS16.0 software. The Student *t* test was used to determine statistical differences between treatment and control values, and *p* < 0.05 was considered significant.

Results

Qu-induced apoptosis in ovarian cancer cells

The cytotoxic effects of Qu on the OC cell line CaOV3 and primary OC cells P#1 were determined with MTT assays after treatment for 48 h. The growth inhibition of Qu in OC cells occurred in a dose-dependent manner. The IC₅₀ values of Qu against CAOV3 and P#1 cells were approximately 40 and 80 μ M, respectively (Fig. 1a). In addition, the apoptotic effect of Qu was determined by Annexin V/PI double staining assay. As shown in Fig. 1b, Qu also increased Annexin V activity in CAOV3 and P#1 cells in a dose-dependent manner. Consistent with this result, the colony formation abilities of Qu-treated groups were remarkably declined compared with those of the DMSO-control group (Fig. 1c).

Next, immunoblotting was used to examine whether Qu-induced cell apoptosis was dependent on the mitochondria-pathway. As shown in Fig. 1d, cytochrome C release from the mitochondria was detected after Qu treatment, accompanied with the elevation of cleaved caspase-9 and cleaved caspase-3. Moreover, Z-VAD-fmk, a pan-caspase inhibitor

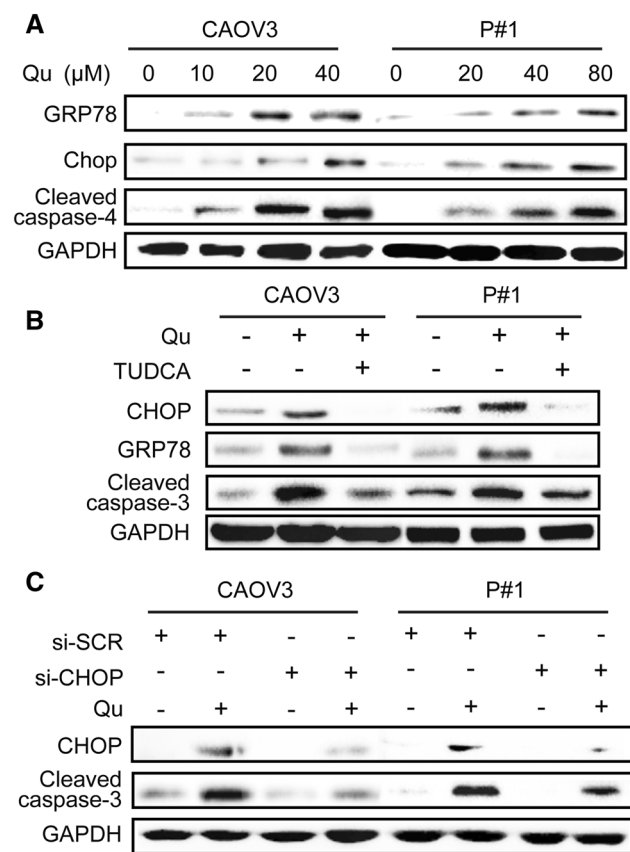


Fig. 2 Qu-induced ER stress mediated caspase-cleavage. **a** CAOV3 and P#1 were exposed to various dosages of Qu, lysates were immunoblotted for GRP78, CHOP and caspase-4 antibodies. **b** CAOV3 and P#1 were treated with DMSO (0.1%), Qu (40 μ M for CAOV3 and 80 μ M for P#1) in the absence or presence of 500 μ M TUDCA for 48 h, respectively, lysates were harvested and immunoblotted with GRP78, CHOP and cleaved caspase-3 antibodies. **c** CAOV3 and P#1 cells were transfected with NC siRNA or CHOP-siRNA and exposed to Qu (40 μ M for CAOV3 and 80 μ M for P#1) for 48 h, western blot analysis of CHOP and cleaved caspase-3. The results were similar in at least three independent experiments

could reverse the apoptotic effect of Qu in ovarian cancer cells, which further confirmed the involvement of the caspase cascade (Fig. 1e). These results indicated that Qu-induced apoptosis in ovarian cancer cells occurred through the mitochondria intrinsic pathway and caspase-dependent.

Qu-induced ER stress contributed to caspase-cleavage

What other cellular responses associated with cell death involved Qu-induced apoptosis? We focused on ER stress, which was a newly discovered apoptosis-related pathway besides the well-recognized death receptor signaling pathway and mitochondrial pathway. Previous studies confirmed Qu could evoke ER stress, which involved cell death in pancreatic and prostate carcinoma cell lines [16, 17], and in our previous studies, we presented evidence that

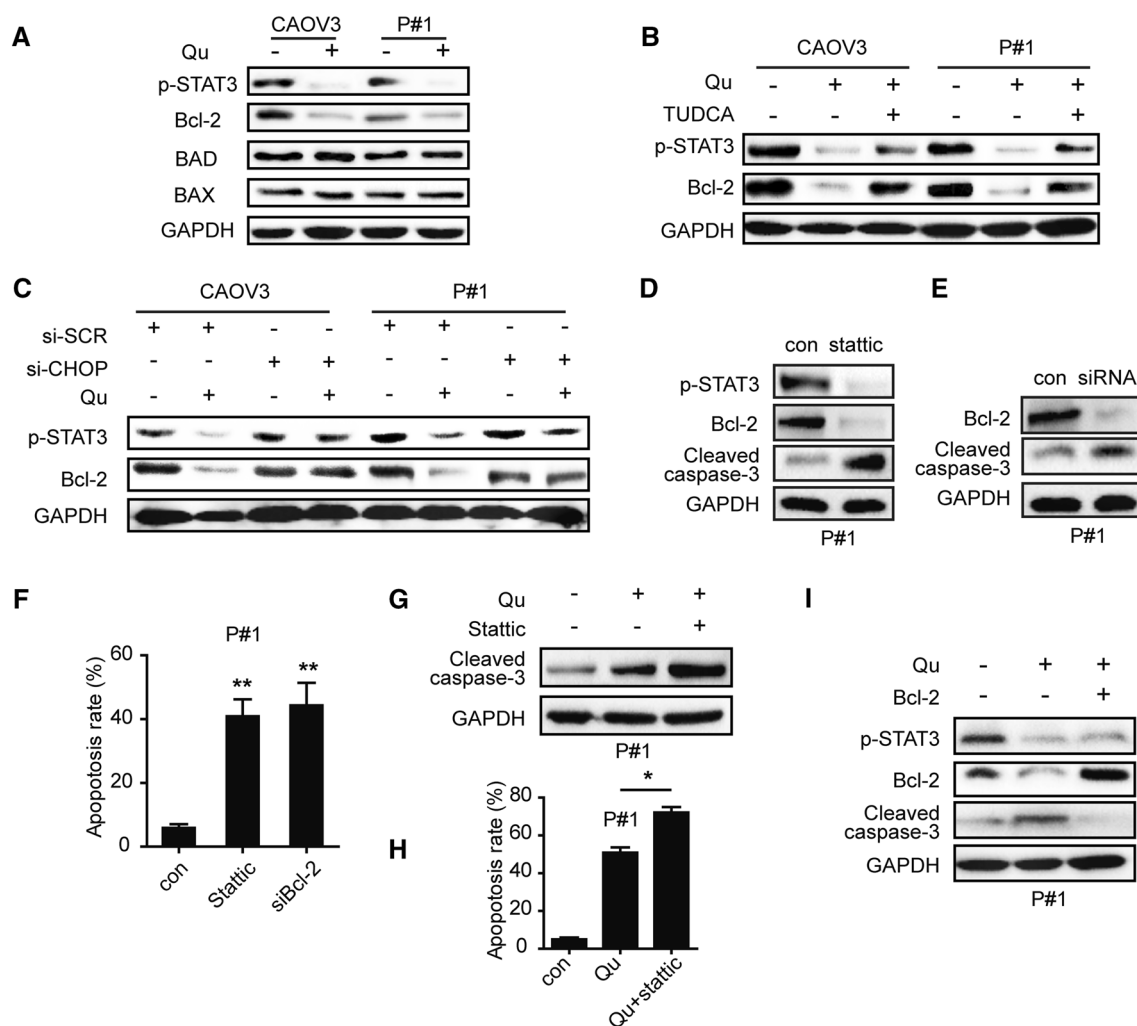


Fig. 3 p-STAT3/Bcl-2 axis participated in Qu-induced ER stress mediating caspase-cleavage. **a** CAOV3 and P#1 cells were incubated with Qu (40 μ M for CAOV3 and 80 μ M for P#1) for 48 h, western blot analysis of p-STAT3 (Tyr705), Bcl-2, BAX and BAD. **b** CAOV3 and P#1 were treated with DMSO (0.1%), Qu (40 μ M for CAOV3 and 80 μ M for P#1) in the absence or presence of 500 μ M TUDCA for 48 h, respectively, western blot analysis of p-STAT3 (Tyr705) and Bcl-2. **c** CAOV3 and P#1 cells were transfected with NC siRNA or CHOP-siRNA and exposed to Qu (40 μ M for CAOV3 and 80 μ M for P#1) for 48 h, western blot analysis of p-STAT3 (Tyr705) and Bcl-2. **d** A specific STAT3 inhibitor static was added to CAOV3 cells for 48 h, western blot analysis of p-STAT3 (Tyr705), Bcl-2 and cleaved

caspase-3. **e** CAOV3 cells were transfected with Bcl-2 specific siRNA for 48 h, western blot analysis of Bcl-2 and cleaved caspase-3. **f** CAOV3 cells were treated as (**d**) and (**e**), Annexin V/PI assay was used to determine the apoptosis rate by flow cytometry. **g**, **h** CAOV3 was treated with Qu (40 μ M) and static for 48 h. **g** Lysates were harvested and immunoblotted with cleaved caspase-3 and GAPDH. **h** Annexin V/PI assay was used to determine the apoptosis rate by flow cytometry. **i** CAOV3 cells were transfected with Bcl-2 plasmid for 48 h, western blot analysis of p-STAT3, Bcl-2 and cleaved caspase-3. The results were similar in at least three independent experiments. * $p < 0.05$. ** $p < 0.01$

Qu triggered ER stress through all three arms to enhance drug cytotoxicity in OC cells. GRP78 is the more abundant ER chaperone and, in addition to its key role in the protein folding process, plays a preeminent role in the regulation of the UPR [18]. CHOP is a transcription factor implicated in the control of translation and apoptosis and the downstream target of three branches of ER stress [19]. Therefore, GRP78 and CHOP were chosen as markers of ER stress in the next study. Recent studies have shown that caspase-4, an ER-resident caspase, was activated in response to ER

stress. Protein expression analysis showed that Qu up-regulated GRP78 and CHOP and led to the cleavage of caspase-4 in CAOV3 and P#1 cells (Fig. 2a), which indicated that the ER stress-associated apoptosis pathway might contribute to Qu-induced OC cell death. Pan-caspase inhibitor could abrogate the cleavage of Caspase-4 after Qu treatment. (Figure S1A).

Tauroursodeoxycholic acid (TUDCA), a classical chemical chaperone against ER stress, was enrolled to relieve ER stress [10]. As shown in Fig. 2b, TUDCA was

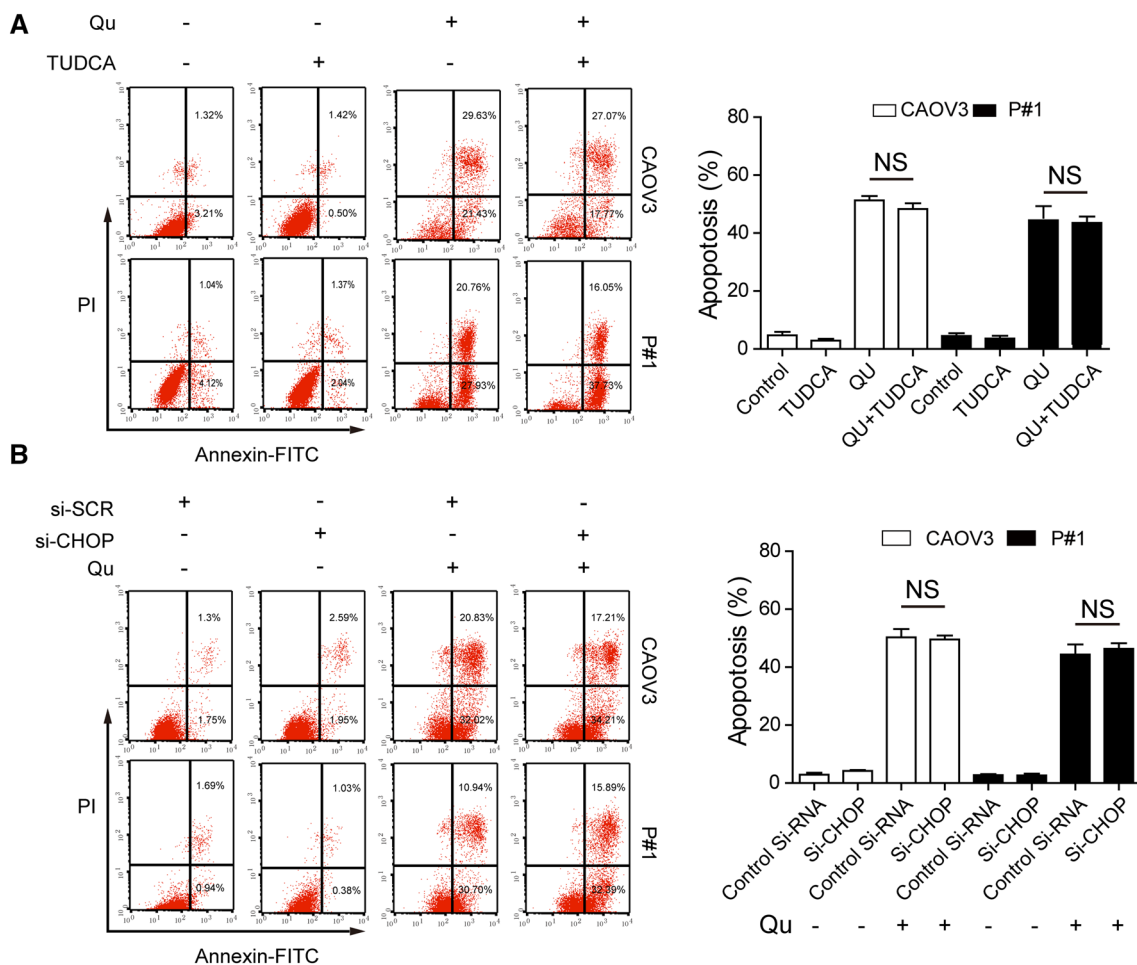


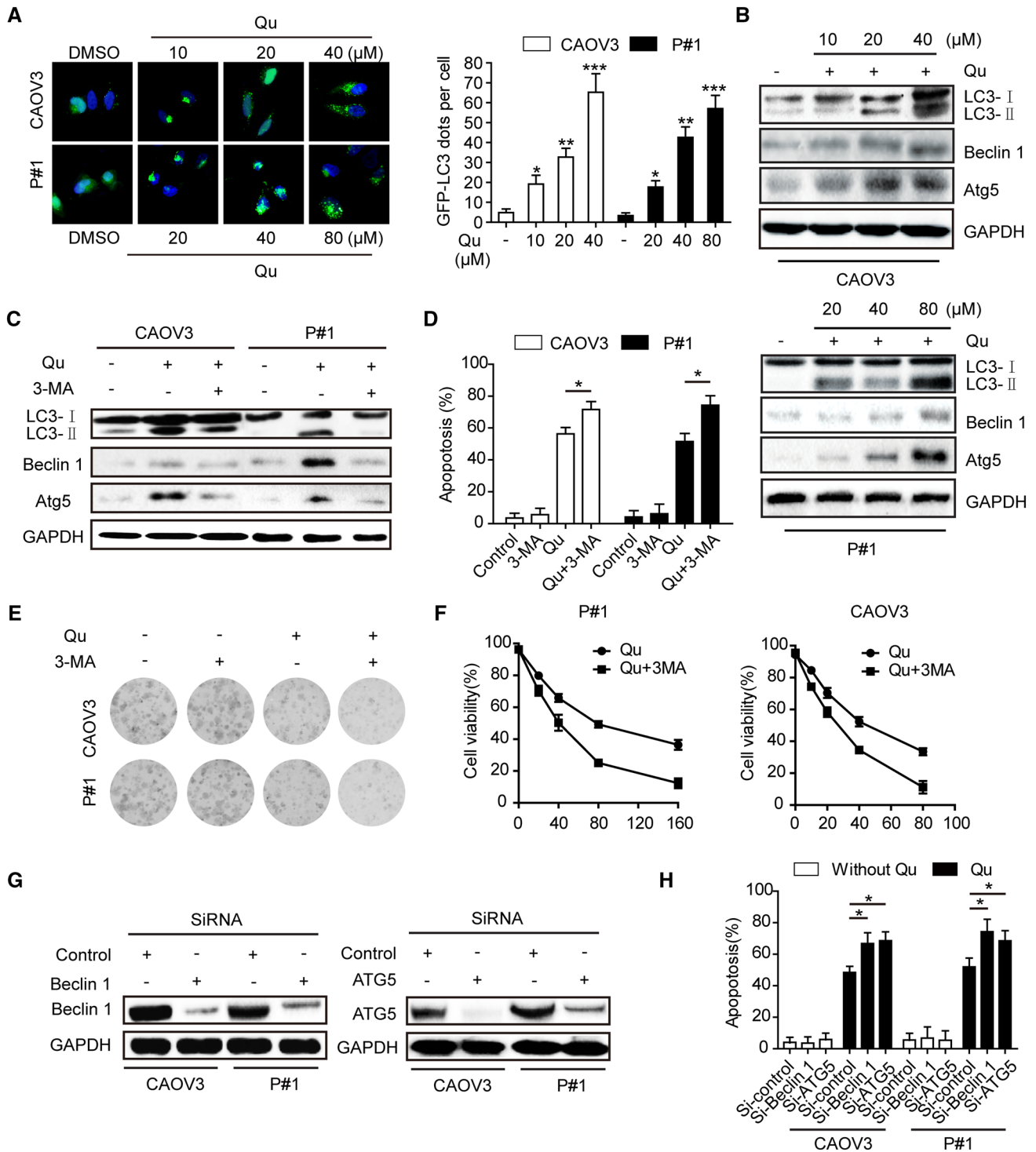
Fig. 4 Inhibition of ER stress could not reverse quercetin-induced apoptosis in ovarian cancer cells. **a** CAOV3 and P#1 were treated with DMSO (0.1%), Qu (40 μ M for CAOV3 and 80 μ M for P#1) in the absence or presence of 500 μ M TUDCA for 48 h, Annexin V/PI assay was used to determine the apoptosis rate by flow cytometry. **b**

CAOV3 and P#1 cells were transfected with NC siRNA or CHOP-siRNA and exposed to Qu (40 μ M for CAOV3 and 80 μ M for P#1) for 48 h, Annexin V/FITC assay was used to determine the apoptosis rate by flow cytometry. The results were similar in at least three independent experiments

sufficient to reverse Qu-induced ER stress in OC cells; meanwhile, it could also decreased the cleavage of caspase 3 under Qu intervention. As CHOP was the best characterized mediator in the transition of ER stress to apoptosis and acted as a key pro-apoptotic transcription factor during ER stress response, we transfected CHOP specific siRNAs in OC cells to clarify whether CHOP contributed to the activity of caspase 3. As expected, Qu-induced upmodulation of CHOP was abolished in the presence of CHOP siRNAs and, notably, partially restored the activation of apoptotic effector caspase 3 (Fig. 2c). Altogether, these results indicated that Qu-induced ER stress was involved in the mitochondrial pathway-mediated apoptosis.

p-STAT3/Bcl-2 axis participated in Qu-induced ER stress mediating apoptosis

To further investigate the mechanism of Qu-induced ER stress and apoptosis, we focused on the p-STAT3/Bcl-2 axis, which was confirmed to be capable of regulating caspase-cleavage to decrease apoptosis [20]. Consistent with our previous studies, the expression of p-STAT3 and Bcl-2 were decreased in CAOV3 and P#1 by Qu. These were not changed by BAX or BAD after Qu treatment (Fig. 3a). Moreover, the supplement of TUDCA or specific CHOP siRNA further supported the connection of ER stress and the inactivation of the p-STAT3/Bcl-2 axis in OC cells (Fig. 3b, c). To further elucidate the connection between p-STAT3/Bcl-2 axis and caspase 3 activity in OC cells, we used a specific STAT3 inhibitor stattic to inactivate the STAT3 pathway or Bcl-2 specific siRNA to knock down the



expression of Bcl-2; as a consequence, cleaved-caspase 3 was notably increased (Fig. 3d, e) and the apoptosis rate of cells was evidently increased (Fig. 3f). In addition, the cells treated with both static and Qu could induce stronger caspase-3 activation and apoptosis than Qu alone (Fig. 3g, h). Finally, CAOV3 cells were transfected with Bcl-2 plasmid

for overexpression of Bcl-2; as a consequence, the activation of cleaved caspase-3 by Qu treatment was abrogated, but p-STAT3 was not influenced (Fig. 3i). Together these results showed that Qu-induced ER stress participated in the mitochondrial apoptosis pathway through the p-STAT3/Bcl-2 axis.

Fig. 5 Qu-induced protective autophagy in ovarian cancer cells. **a** CAOV3 and P#1 cells transfected with pEGFP-LC3 plasmid were treated with DMSO (<0.1%) or different concentrations of Qu for 48 h. The average number of dots per positive cell were counted. **b** Lysates of CAOV3 and P#1 cells were harvested and immunoblotted with LC3, Beclin 1 and Atg5 after treatment with various concentrations of Qu for 48 h. **c–f** Cells were incubated with DMSO (<0.1%), Qu (40 μ M for CAOV3 cells and 80 μ M for P#1 cells) in the absence or presence of 3MA (10 mM) for 48 h. **c** Western blot analysis of LC3, Beclin 1 and Atg5. **d** The apoptotic rate was analyzed by flow cytometry. **e** The effect of growth inhibition was measured by the violet staining assay, and photographs were shown at 14 days. **f** The cell viability rate was assessed using the CCK8 assay comparing quercetin only and the combination of quercetin and 3MA. **g** Detection of the inhibition efficiency for siRNAs against ATG5 or Beclin1. CAOV3 and P#1 cells were transfected with siRNAs targeting ATG5 or Beclin1 for 48 h, western blot analysis of Beclin1 and Atg5. **h** Cells were transfected with NC siRNA, ATG5 or Beclin1-siRNA in the absence or presence of Qu (40 μ M for CAOV3 cells and 80 μ M for P#1 cells) for 48 h, and apoptosis rates were analyzed by flow cytometry. The results were similar in at least three independent experiments. * $p < 0.05$; ** $p < 0.01$

Inhibition of ER stress could not reverse quercetin-induced apoptosis

Unexpectedly, neither adding TUDCA nor knocking down CHOP could abolish Qu-induced apoptosis in CAOV3 and P#1 cells (Fig. 4a, b), which suggested that Qu-induced ER stress might act by a function other than the mediating mitochondrial apoptosis pathway.

Qu-induced protective autophagy in ovarian cancer cells

To determine the above phenomenon and to better understand the exact role of Qu-induced ER stress, we examined other cellular responses associated with cell death after Qu treatment. Recently, a growing body of evidence demonstrated that autophagy is associated with both survival or apoptotic processes in cells dependent on various stimulus conditions [21, 22]. Electron microscopy analysis of Qu-treated cells highlighted the presence of double membrane vacuolar structures with the morphological features of autophagosomes in the cytoplasm of both CAOV3 and P#1 cells (data not shown). To further confirm this result, GFP-MAPLC3B plasmids were stably transfected into CAOV3 and P#1 cells to generate these two constitutively expressing GFP-LC3B cell lines. Fluorescence microscopy allowed us to monitor autophagy by identifying punctate GFP-LC3B in GFP-LC3B-CAOV3 and GFP-LC3B-P#1 cells exposed to Qu at various concentrations. As shown in Fig. 5a, Qu-treated CAOV3 and P#1 cells displayed a significant increase in the density of GFP-LC3B dots in a dose dependent manner. Immunoblot also revealed that Qu led to an enhanced LC3B conversion in a dose dependent

manner, and autophagy-associated genes Beclin 1 and Atg5 were also activated (Fig. 5b).

To investigate the role of Qu-induced autophagy on apoptosis in ovarian cancer, we used the autophagy scavenger 3-MA in combination with Qu. As shown in Figs. 5c–f, 3MA effectively abrogated Qu-induced LC3B turnover and the expression of ATG5 and Beclin 1, resulting in enhanced cytotoxicity of Qu to CAOV3 and P#1 cells. In addition, silencing the expression of either Atg5 or Beclin 1 could also aggravate Qu-induced cell death (Fig. 5g, h). Above all, these results suggested that Qu-induced autophagy might play a protective role in ovarian cancer cells.

Qu-induced ER stress mediated autophagy

The close relationship between ER stress and autophagy has been demonstrated by recent reports showing that ER stress is a potent inducer of autophagy [23]. To investigate whether ER stress following Qu treatment generated an autophagic response, western blotting was performed to probe the expression of LC3B, ATG5 and Beclin 1. TUDCA addition or knocking down CHOP could attenuate the expression of LC3B, ATG5 and Beclin 1 induced by Qu (Fig. 6a, b). CHOP is the downstream target for three branches of ER stress, and the three branches were examined using inhibitors [9]. As shown in Figure S2A–C, all three branches of ER stress could regulate autophagy response. These results demonstrated that Qu-induced autophagy was ER stress dependent in OC cells. Moreover, 3-MA could not alter the expression of GRP78 or CHOP induced by Qu, suggesting that autophagy acted downstream of ER stress after Qu treatment (Fig. 6c). To further explore the potential correlation between ER stress and autophagy in ovarian cancer, the mRNA data of GRP78, ATG5 and Beclin 1 from 594 ovarian cancer specimens was obtained from the TCGA database. As shown in Fig. 6d, the Spearman correlation analysis on the normalized mRNA expression value revealed that the GRP78 expression level was positively correlated with that of ATG5 ($R = 0.143$, $p < 0.001$) and BECN1 ($R = 0.293$, $p < 0.001$). This underlying positive correlation of ER stress and the autophagy markers implied a possible dominating relationship between ER stress signaling and the autophagy response.

p-STAT3/Bcl-2 axis participated in Qu-induced ER stress mediating autophagy

Beclin1, a Bcl-2-homology (BH)-3 domain-only protein, interacts with Bcl-2, stabilizes the Beclin1 homodimer, and suppresses autophagy [24]. In addition, the Bcl-2 family proteins are closely related to the IRE1/JNK pathway, which also participates in ER stress-mediated

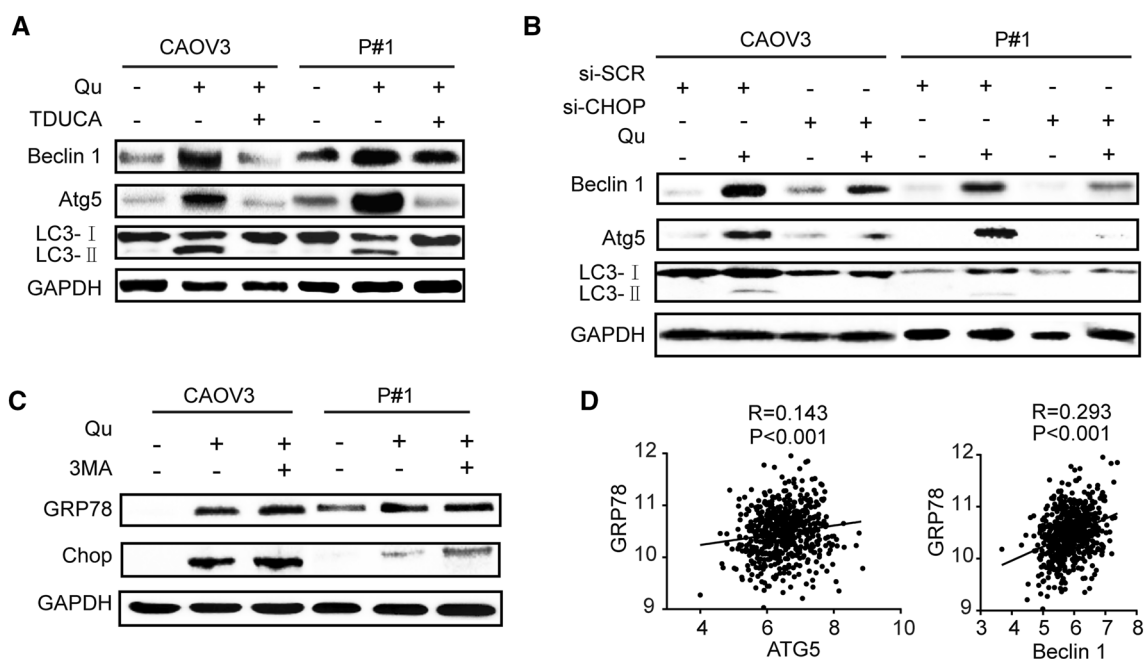


Fig. 6 Qu-induced autophagy dependent of ER stress in ovarian cancer. **a** CAOV3 and P#1 cells were treated with DMSO (<0.1%), Qu (40 μ M for CAOV3 cells and 80 μ M for P#1 cells) or Qu in combination with TUDCA (500 μ M) for 48 h, lysates were harvested and immunoblotted with LC3, Beclin 1 and Atg5. **b** CAOV3 and P#1 cells were transfected with NC siRNA or CHOP-siRNA and exposed to Qu (40 μ M for CAOV3 and 80 μ M for P#1) for 48 h, western blot

analysis of LC3, Beclin 1 and Atg5. **c** CAOV3 and P#1 cells were treated with DMSO (<0.1%), Qu (40 μ M for CAOV3 cells and 80 μ M for P#1 cells) or Qu in combination with 3MA (10 mM) for 48 h, Western blot analysis of GRP78 and CHOP. **d** Using the normalized mRNA data of 594 ovarian cancer specimens obtained from the TCGA database gene, a Spearman correlation was performed between GRP78 gene expression with that of ATG5 and Beclin1

autophagy [25]. Co-immunoprecipitation was used to validate this interaction of Bcl-2 and Beclin 1 after Qu administration. Consistent with previous reports, Beclin 1 and Bcl-2 co-immunoprecipitation with each other was markedly decreased in Qu-treated OC cells [15].

To further investigate the connection between Bcl-2 and Beclin 1 in ovarian cancer cells, we knocked down the expression of Bcl-2; as a consequence, Beclin 1 was notably increased accordingly. In parallel, static also increased the expression of Beclin 1 in OC cells (Fig. 7b,

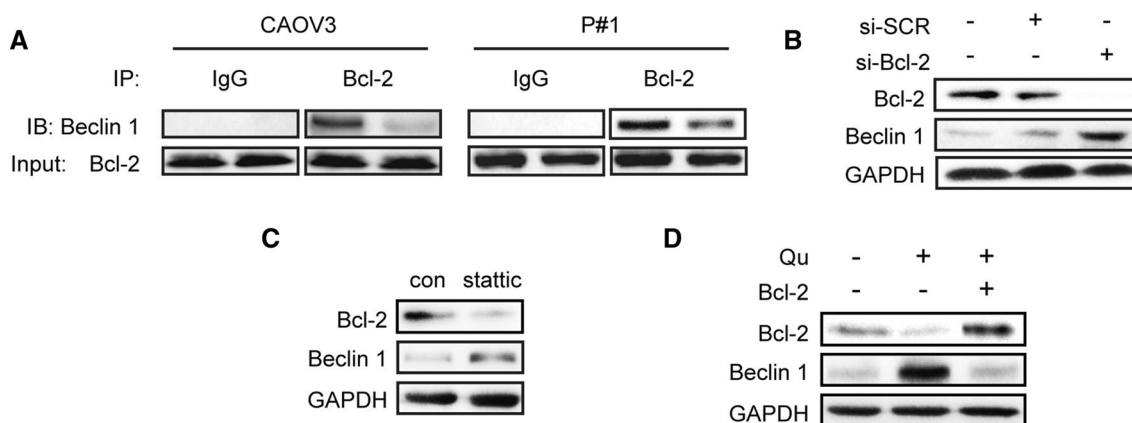


Fig. 7 The role of the p-STAT3/Bcl-2 axis in quercetin-induced autophagy. **a** Co-immunoprecipitation analysis of Beclin 1 and Bcl-2 from lysates of CAOV3 and P#1 cells treated with DMSO (<0.1%) or Qu (40 μ M for CAOV3 cells and 80 μ M for P#1 cells). **b** CAOV3 cells was transfected with Bcl-2 specific siRNA for 48 h, Western blot

analysis of Bcl-2 and Beclin 1. **c** The specific STAT3 inhibitor static was added to CAOV3 cells for 48 h, western blot analysis of Bcl-2 and Beclin 1. **d** CAOV3 cells were transfected with Bcl-2 plasmid for 48 h, western blot analysis of, Bcl-2, Beclin 1 and GAPDH. The results were similar in at least three independent experiments

c). Finally, CAOV3 cells were transfected with a Bcl-2 plasmid to overexpress Bcl-2; as a consequence, Beclin 1 increased after Qu treatment was abrogated (Fig. 7d). Taken together, these results showed that Qu-induced ER stress was involved in protective autophagy responses in ovarian cancer via the p-STAT3/Bcl-2 axis.

3-MA could enhance Qu’s anticancer effect in a CAOV3 xenograft model

To further investigate whether inhibition of autophagy could sensitize Qu’s anticancer effect in vivo, a mouse xenograft ovarian cancer model was established by i.p. injection of 5×10^6 CAOV3 human OC cells into female NOD/SCID mice. As shown in Fig. 8a, b, i.p. injections

of Qu in combination with 3-MA resulted in a remarkable reduction of abdominal tumor burden compared with the solitary intervention group with Qu or 3-MA only. Moreover, administration of Qu in combination with 3-MA strikingly prolonged survival compared with that of other groups ($p < 0.01$) (Fig. 8c). We found the same results in a time course xenograft model (Fig. 8d). After measuring the last tumor using in vivo bioluminescence images, the mice were sacrificed and the tumor masses were obtained and analyzed by immunohistochemistry. In accordance with the in vitro results, GRP78, Beclin 1 and cleaved caspase-3 expression was increased in the Qu-treatment groups, indicating ER stress and autophagy were activated under Qu intervention. However, Qu in combination with

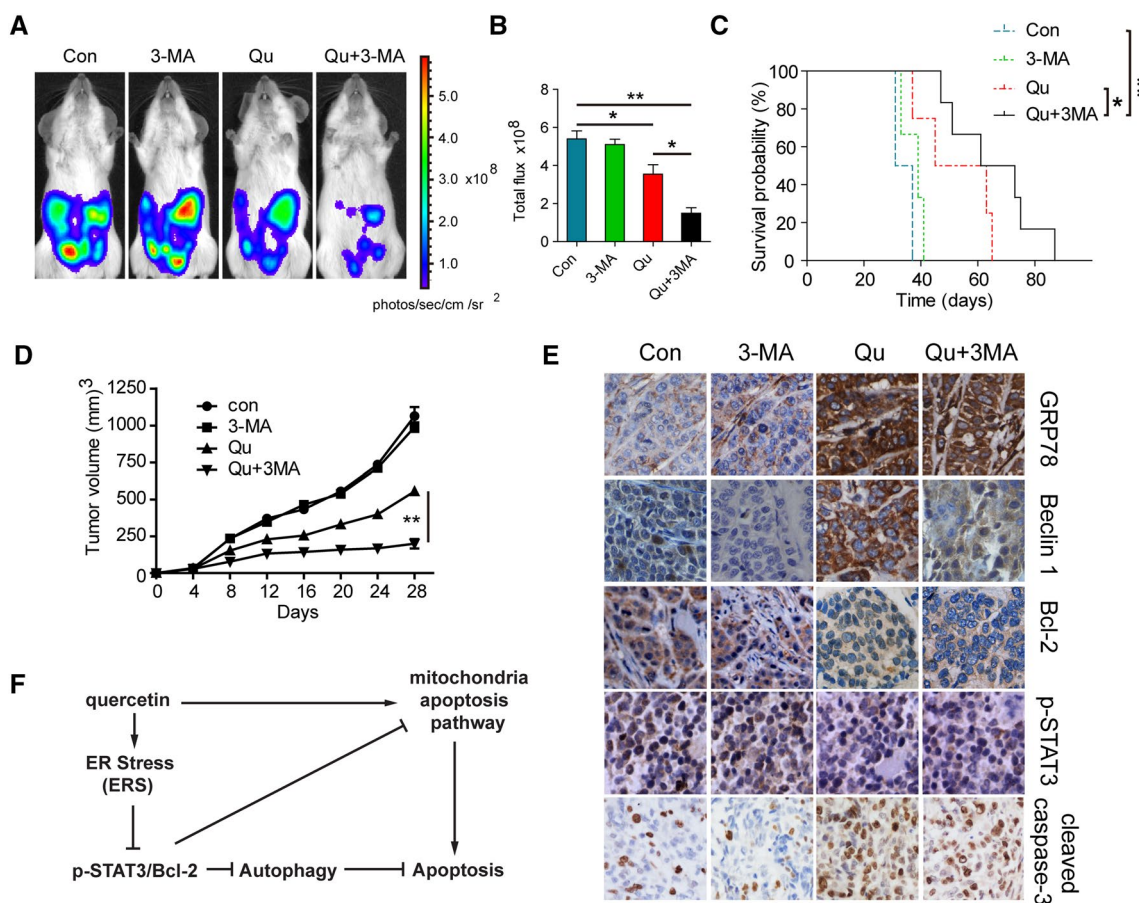


Fig. 8 Inhibition of autophagy enhances Qu’s anticancer effects in a CAOV3 xenograft model. **a, b** NOD/SCID mice were inoculated with CAOV3 cells via intraperitoneal injection (i.p.), and then randomly divided into four groups. The next day, the four mouse groups were treated with saline, 3MA (30 mg/Kg, i.p.), Qu (80 mg/Kg, i.p.) or Qu+3MA respectively, respectively. The abdominal cavity tumor burden in the mice was assayed by in vivo bioluminescence imaging. Representative images of mice were shown **a** bioluminescence signal was measured for regions of interest and normalized as total flux (**b**, n=8 per group). **c** Kaplan–Meier survival curves demonstrated the

survival status in each treatment group (n=8 per group). **d** CAOV3 cell-derived tumors developed in NOD/SCID mice and treated with saline, 3MA (30 mg/Kg, i.p.), Qu (80 mg/Kg, i.p.) or Qu+3MA. Tumor growth was monitored by measuring the tumor volume for 4 weeks. (n=6 mice per group). **e** Tumor samples were subjected to immunohistochemical analysis of GRP78, Beclin 1, p-STAT3, cleaved caspase-3 and Bcl-2 ($\times 200$). **f** Schematic model illustrating the potential pathway associated with Qu-induced ER stress in ovarian cancer cells. * $p < 0.05$; ** $p < 0.01$

3-MA obviously reduced Beclin 1 compared to that of mice treated with Qu alone ($p < 0.05$) (Fig. 8e).

Discussion

Epithelial OC is the most common cause of death among gynecological malignancies. Despite cytoreductive surgery and systemic chemotherapy showing rapid effects during the initial treatment, most patients unavoidably experience disease recurrence within two years, which led to the dismal prognosis of OC patients. Therefore, it is urgent to find alternative therapies or new regimen to enhance the removal of OC cells. Targeting the ER stress pathway is recently being regarded as a promising new strategy for drug discovery and cancer therapy. Because prolonged or irreversible ER stress can lead to cell death, this pathway has potential for anticancer therapy [26]. Qu, a common natural flavonoid in many fruits and vegetables, screened out as a potent ER stress inducer from thousands of varieties of flavonoids, could increase IRE1 nuclease activity and splicing of XBP1 [27] and has been shown to induce ER stress by enhancing apoptosis in prostate, glioma, pancreatic, and colon cancer cells [16, 17, 28], thus showing a variety of anticancer effects in many cancer cells.

In this study, we provided prudent evidence that Qu evoked ER stress by directly inducing apoptosis through elevated levels of GRP78, CHOP and cleaved caspase 4 after Qu treatment inCAOV3 and primary OC cells. Caspase 4 has been identified as a key player in ER-induced apoptosis [29]. As a support, cells treated with siRNA targeting caspase 4 were resistant to ER-stress-induced apoptosis [30]. Further functional analysis showed that inhibition of ER stress by TUDCA addition or knocking down CHOP partially reversed the activation of apoptotic effector caspase 3, which further supports the view that Qu-induced ER stress leads to apoptosis. In a previous study, we demonstrated that Qu selectively suppressed constitutive STAT3 phosphorylation and down-regulated the expression of the STAT3-regulated gene Bcl-2 [9]. Bcl-2, a crucial anti-apoptosis element, was confirmed to negatively regulate the mitochondrial-apoptosis pathway [31]. Knocking down Bcl-2 could increase the cleavage of caspase 3 in OC, which indicates that the decrease of Bcl-2 exerted by Qu was actually responsible for the apoptosis. Moreover, we found the same results in static-treatment experiments. Bcl-2 rescue experiments demonstrated the opposite result. These data clarified that Qu-induced ER stress participated in cellular apoptosis via the p-STAT3/Bcl-2 axis.

Conversely, other researchers showed that Qu exerted protective effects by decreasing ER stress in normal cells including intestinal epithelial cells and endothelial cells [32, 33]. Our study found that Qu could not evoke ER stress

or apoptosis in normal ovarian cells, HOSE, even at high doses such as 80 μ M (Figure S3A and B). This discriminative effect exerted by Qu between normal and cancer cells is still not clear, which thus shows Qu to be an excellent anticancer candidate in OC through ER stress.

Intriguingly, inhibition of ER stress could not reverse Qu-induced apoptosis, suggesting there was another compensational biological behavior associated with this process. In this study, we focused on autophagy for the following reasons. First, autophagy can be evoked in tumor cells by a variety of stress signals such as nutrient starvation or anticancer agents treatment [34]. The data presented here showed that Qu induces autophagy in ovarian cancer cells. We demonstrated that Qu increases the number and density of GFP-LC3B dots and enhances LC3-II formation and LC3B conversion, a classical marker of autophagy, and increases the expression of other autophagy related genes such as ATG5 and Beclin1. This phenomenon was further confirmed by in vivo experiments because increased Beclin-1 was seen through IHC after the addition of Qu. Second, autophagy was involved in the promotion or inhibition of cancer cell survival in various situations [35, 36], thus affecting the fate of treated cells. Here, functional analysis showed that either blocking the upstream pathway of autophagy flux with 3-MA or specially knocking down ATG5 and Beclin1 with siRNA markedly amplified Qu-induced apoptotic cell death, which was further confirmed by in vivo tumor xenograft models that showed 3-MA to strengthen the anticancer effects of Qu, indicating that Qu-induced autophagy played a protective role in OC cells.

The link between ER stress and autophagy was only began to be investigated from last decade, and many questions about the signaling pathways concerning ER stress with autophagy remain largely un-answered. This study presented the first evidence that Qu-evoked ER stress induces protective autophagy in OC cells, and the p-STAT3/Bcl-2 axis is the linker contributing to ER stress-mediated autophagy. First, TUDCA or reducing expression of CHOP abrogates the LC3-II, ATG5 and Beclin 1 elevation exerted by Qu treatment in ovarian cells. Alternatively, the autophagy inhibitor 3-MA in combination with Qu did not alter the expression of GRP78 or CHOP, suggesting that autophagy acted downstream of ER stress after Qu treatment. Second, Spearman correlation analysis of 594 OC specimens from the TCGA database showed positive correlations between ER stress and autophagy markers, and other research has demonstrated the expression of the autophagy-related gene Beclin 1 being inversely correlated with the expression of Bcl-2 in clinical ovarian carcinoma specimens by immunohistochemistry [37], indicating the possible dominating relationship between ER stress signaling and the autophagy response. Third, the co-immunoprecipitation

results in this study demonstrated that the interaction of Beclin 1 with Bcl-2 in ovarian cancer cells was dissociated after Qu treatment. Furthermore, knocking down Bcl-2 or static-addition, resembling induction by Qu, increases the expression of Beclin 1 in ovarian cancer. Finally, Bcl-2 overexpression abrogates the increased expression of Beclin 1 by Qu treatment. These results indicate that the p-STAT3/Bcl-2 axis contributes to ER stress-mediated autophagy. This phenomena could explain the reason inhibiting autophagy with 3-MA sensitizes Qu-induced cell death because Qu-induced ER stress activates protective autophagy at the same time and in the same manner as it activates the p-STAT3/Bcl-2 axis, leading to the same outcome.

Increasing number of scholars believe that targeting to the ER stress is a new strategy for drug discovery and cancer therapy. In previous study, we demonstrated that Qu could evoke ER stress to influence p-STAT3/Bcl-2 to enhance the drug cytotoxicity. In this research, we further unveiled the effect of Qu-induced ER stress on the survival in ovarian cancer cells by itself. We first demonstrated that ER stress was involved in mediating mitochondrial-mediated apoptosis and protective autophagy at the same time. Interestingly, the p-STAT3/Bcl-2 axis also took part in this process. The results provided a new explanation for protective Autophagy induced by quercetin, and providing a new angle to consider in clinical studies of biological modifiers that circumvent drug resistance in patients by targeting the ER stress pathway.

Acknowledgements Grant support: Educational Commission of Hubei Province of China (No. B2016078) National Science Foundation of China (No. 81072135, 81372801, 81272426, 81572570) and the “973” Program of China (No. 2015CB553903) supported this work.

Author contributions YL, WG and ZYY contributed equally to this work.

Conflict of interest The authors have no conflict of interest.

References

- Mitra AK, Sawada K, Tiwari P, Mui K, Gwin K, Lengyel E (2011) Ligand-independent activation of c-Met by fibronectin and alpha(5)beta(1)-integrin regulates ovarian cancer invasion and metastasis. *Oncogene* 30:1566–1576
- Bast RC Jr, Hennessy B, Mills GB (2009) The biology of ovarian cancer: new opportunities for translation. *Nat Rev Cancer* 9:415–428
- De A, De A, Papisian C et al (2013) Emblica officinalis extract induces autophagy and inhibits human ovarian cancer cell proliferation, angiogenesis, growth of mouse xenograft tumors. *PLoS One* 8:e72748
- Song NR, Chung MY, Kang NJ et al (2014) Quercetin suppresses invasion and migration of H-Ras-transformed MCF10A human epithelial cells by inhibiting phosphatidylinositol 3-kinase. *Food Chem* 142:66–71
- Del Follo-Martinez A, Banerjee N, Li X, Safe S, Mertens-Talcott S (2013) Resveratrol and quercetin in combination have anticancer activity in colon cancer cells and repress oncogenic micro-RNA-27a. *Nutr Cancer* 65:494–504
- Gates MA, Vitonis AF, Tworoger SS et al (2009) Flavonoid intake and ovarian cancer risk in a population-based case-control study. *Int J Cancer* 124:1918–1925
- Kim I, Xu W, Reed JC (2008) Cell death and endoplasmic reticulum stress: disease relevance and therapeutic opportunities. *Nat Rev Drug Discov* 7:1013–1030.
- Sano R, Reed JC (2013) ER stress-induced cell death mechanisms. *Biochim Biophys Acta* 1833:3460–3470
- Yang Z, Liu Y, Liao J et al (2015) Quercetin induces endoplasmic reticulum stress to enhance cDDP cytotoxicity in ovarian cancer: involvement of STAT3 signaling. *FEBS J* 282:1111–1125
- Yi L, Zongyuan Y, Cheng G, Lingyun Z, Guilian Y, Wei G (2014) Quercetin enhances apoptotic effect of tumor necrosis factor-related apoptosis-inducing ligand (TRAIL) in ovarian cancer cells through reactive oxygen species (ROS) mediated CCAAT enhancer-binding protein homologous protein (CHOP)-death receptor 5 pathway. *Cancer Sci* 105:520–527
- Rabinowitz JD, White E (2010) Autophagy and metabolism. *Science* 330:1344–1348
- Wei Y, Sinha S, Levine B (2008) Dual role of JNK1-mediated phosphorylation of Bcl-2 in autophagy and apoptosis regulation. *Autophagy* 4:949–951
- Zhou Y, Liang X, Chang H et al (2014) Ampelopsin-induced autophagy protects breast cancer cells from apoptosis through Akt-mTOR pathway via endoplasmic reticulum stress. *Cancer Sci* 105:1279–1287
- Zhao X, Fang Y, Yang Y et al (2015) Elaiophylin, a novel autophagy inhibitor, exerts antitumor activity as a single agent in ovarian cancer cells. *Autophagy* 11:1849–1863
- Wang K, Liu R, Li J et al (2011) Quercetin induces protective autophagy in gastric cancer cells: involvement of Akt-mTOR- and hypoxia-induced factor 1alpha-mediated signaling. *Autophagy* 7:966–978
- Lee JH, Lee HB, Jung GO, Oh JT, Park DE, Chae KM (2013) Effect of quercetin on apoptosis of PANC-1 cells. *J Korean Surg Soc* 85:249–260
- Liu KC, Yen CY, Wu RS et al (2014) The roles of endoplasmic reticulum stress and mitochondrial apoptotic signaling pathway in quercetin-mediated cell death of human prostate cancer PC-3 cells. *Environ Toxicol* 29:428–439
- Ulianich L, Insabato L (2014) Endoplasmic reticulum stress in endometrial cancer. *Front Med* 1:55
- Chistiakov DA, Sobenin IA, Orekhov AN, Bobryshev YV (2014) Role of endoplasmic reticulum stress in atherosclerosis and diabetic macrovascular complications. *BioMed Res Int* 2014:610140
- Duan W, Yang Y, Yi W et al (2013) New role of JAK2/STAT3 signaling in endothelial cell oxidative stress injury and protective effect of melatonin. *PLoS One* 8:e57941
- Shi Y, Tang B, Yu PW et al (2012) Autophagy protects against oxaliplatin-induced cell death via ER stress and ROS in Caco-2 cells. *PLoS One* 7:e51076
- Warr MR, Binnewies M, Flach J et al (2013) FOXO3A directs a protective autophagy program in haematopoietic stem cells. *Nature* 494:323–327

23. Ma XH, Piao SF, Dey S et al (2014) Targeting ER stress-induced autophagy overcomes BRAF inhibitor resistance in melanoma. *J Clin Invest* 124:1406–1417
24. Maejima Y, Kyoji S, Zhai P et al (2013) Mst1 inhibits autophagy by promoting the interaction between Beclin1 and Bcl-2. *Nat Med* 19:1478–1488
25. Meister S, Frey B, Lang VR et al (2010) Calcium channel blocker verapamil enhances endoplasmic reticulum stress and cell death induced by proteasome inhibition in myeloma cells. *Neoplasia* 12:550–561
26. Verfaillie T, Garg AD, Agostinis P (2013) Targeting ER stress induced apoptosis and inflammation in cancer. *Cancer Lett* 332:249–264
27. Kraskiewicz H, Fitzgerald U (2012) Interfering with endoplasmic reticulum stress. *Trends Pharmacol Sci* 33:53–63
28. Jakubowicz-Gil J, Langner E, Badziul D, Wertel I, Rzeski W (2013) Silencing of Hsp27 and Hsp72 in glioma cells as a tool for programmed cell death induction upon temozolomide and quercetin treatment. *Toxicol Appl Pharmacol* 273:580–589
29. Yamamuro A, Kishino T, Ohshima Y et al (2011) Caspase-4 directly activates caspase-9 in endoplasmic reticulum stress-induced apoptosis in SH-SY5Y cells. *J Pharmacol Sci* 115:239–243
30. Thepparit C, Khakpoor A, Khongwichit S, et al. (2013) Dengue 2 infection of HepG2 liver cells results in endoplasmic reticulum stress and induction of multiple pathways of cell death. *BMC Res Notes* 6:372
31. Hui K, Yang Y, Shi K et al (2014) The p38 MAPK-regulated PKD1/CREB/Bcl-2 pathway contributes to selenite-induced colorectal cancer cell apoptosis in vitro and in vivo. *Cancer Lett* 354:189–199
32. Natsume Y, Ito S, Satsu H, Shimizu M (2009) Protective effect of quercetin on ER stress caused by calcium dynamics dysregulation in intestinal epithelial cells. *Toxicology* 258:164–175
33. Wu J, Xu X, Li Y et al (2014) Quercetin, luteolin and epigallocatechin gallate alleviate TXNIP and NLRP3-mediated inflammation and apoptosis with regulation of AMPK in endothelial cells. *Eur J Pharmacol* 745:59–68
34. Verfaillie T, Salazar M, Velasco G, Agostinis P (2010) Linking ER stress to autophagy: potential implications for cancer therapy. *Int J Cell Biol* 2010:930509
35. Bommareddy A, Hahm ER, Xiao D et al (2009) Atg5 regulates phenethyl isothiocyanate-induced autophagic and apoptotic cell death in human prostate cancer cells. *Cancer Res* 69:3704–3712
36. Chen YJ, Huang WP, Yang YC et al (2009) Platonin induces autophagy-associated cell death in human leukemia cells. *Autophagy* 5:173–183
37. Valente G, Morani F, Nicotra G et al (2014) Expression and clinical significance of the autophagy proteins BECLIN 1 and LC3 in ovarian cancer. *BioMed Res Int* 2014:462658